Molecular Size and Structure of Asphaltene from Various Sources

ARTICLE *in* ENERGY & FUELS · MARCH 2000

Impact Factor: 2.79 · DOI: 10.1021/ef990225z

2 AUTHORS, INCLUDING:

Oliver C Mullins
Schlumberger Limited
244 PUBLICATIONS **5,940** CITATIONS

SEE PROFILE

Molecular Size and Structure of Asphaltenes from Various Sources

Henning Groenzin and Oliver C. Mullins*

Schlumberger-Doll Research, Ridgefield, Connecticut 06877

Received November 2, 1999. Revised Manuscript Received February 10, 2000

Fluorescence depolarization measurements are used to determine the size of asphaltene molecules and of model compounds for comparison. Mean molecular weights of roughly 750 amu with a range of roughly 500−1000 amu are found for petroleum asphaltenes. A strong correlation is established between the size of an individual fused ring system in an asphaltene molecule and the overall size of this corresponding molecule, showing that asphaltene molecules have one or perhaps two fused ring systems per molecule. Subtle differences in molecular size are found for different virgin crude oil asphaltenes and for a vacuum resid asphaltene. Coal asphaltene molecules are found to be much smaller than petroleum asphaltenes. The molecular sizes of resins and asphaltenes are found to form a continuous distribution.

I. Introduction

Asphaltenes occupy a central, if often hindering, role in the utilization of hydrocarbon resources.[1−6] The increase in viscosity in crude oil which accompanies increased asphaltene content coupled with the tendency of asphaltenes to phase separate creates significant difficulties in the production and transportation of crude oil. The coating tendencies of asphaltenes along with their heavy metal content interfere with catalytic processing of crude oils. Other applications of asphaltic materials such as for paving materials[7] or coating materials[8] are strongly affected by the asphaltene content. Despite the impact of asphaltenes in very important economic spheres, some of their most fundamental properties have remained unresolved.

The molecular weight of asphaltenes has been a matter of considerable controversy for 20 years. Various measurements have yielded values which differ by as much as a factor of 10 or more. For instance, field ionization mass spectroscopy results have indicated a molecular weight in the range of 700 amu,[9] while vapor pressure osmometry (VPO) has produced much larger molecular weights for the same asphaltenes, e.g., 4000 amu.[9] The large molecular weights obtained by VPO were explained by evident aggregation of asphaltenes at requisite concentrations. Size exclusion chromatography has yielded average molecular weights as high as ∼10 000 amu.[10] Recent laser desorption mass spectroscopic[11] results have given asphaltene molecular weights of 400 amu (with a range of roughly 200−600 amu) in rough agreement with the FIMS work.[9] Rough agreement here means that there is less than a factor of 2 difference in the average molecular weight as opposed to the one-to-two orders of magnitude difference found among different measurements. The factor of 2 difference may be due in part to different samples. Other laser desorption mass spectral measurements yield a range of ∼250−1200 amu with a mean of about 500 amu for vacuum resid petroleum asphaltenes.[12]

Nevertheless, a widely quoted recently proposed structure of an asphaltene molecule incorporated a molecule weight in excess of 6000 amu.[13] Apparently a consensus has not been reached. Those supporting large molecular weights claim that at least mass spectral measurements suffer from fragmentation and do not volatilize the heaviest ends. There is general agreement that colligative methods such as VPO suffer from aggregate formation; thereby yielding aggregate molecular weights. In addition, chromatographic methods such as gel permeation chromatography have the additional problem of the lack of good standards. However, there is not general agreement as to how debilitating these problems are.

The number of rings in a single asphaltene fused ring system has been another area of uncertainty with early estimates ranging from a few rings to 20. However, a concurrence of results from many different techniques indicate that on average asphaltene ring systems have

* Corresponding author.

(1) *Bitumens, Asphalts, and Tar Sands*; Chilingarian, G. V., Yen, T. F., Eds.; Elsevier Scientific Publishing Co.: New York, 1978.
(2) Speight, J. G. *The Chemistry and Technology of Petroleum*; Marcel Dekker: New York, 1980.
(3) Tissot, B. P.; Welte, D. H. *Petroleum Formation and Occurrence*; Springer-Verlag: Berlin, 1984.
(4) *Chemistry of Asphaltenes*; Bunger, J. W.; Li, N. C., Eds.; American Chemical Society: Washington DC, 1984.
(5) *Asphaltenes, Fundamentals and Applications*; Sheu, E. Y.; Mullins, O. C., Eds.; Plenum Press: New York, 1995.
(6) *Structures and Dynamics of Asphaltenes*; Mullins, O. C., Sheu, E. Y., Eds.; Plenum Press: New York, 1998.
(7) Lin, M. S.; Lunsford, K. M.; Glover, C. J.; Davidson, R. R.; Bullin, J. A. Chapter 5, ref 5.
(8) Lian, H.; Yen, T. F. Chapter 6, ref 5.
(9) Boduszynski, M. W. Chapter 7, ref 4.
(10) Anderson, S. I. *Fuel Sci. Technol. Int*. **1994**, *12*, 51.
(11) Miller, J. T.; Fisher, R. B.; Thiyagarajan, P.; Winans, R. E.; Hunt, J. E. *Energy Fuels* **1998**, *12*, 1290.
(12) Yang, M.-G.; Eser, S. ACS Reprints, ACS New Orleans Meeting, 768, 1999.
(13) Strausz, O. P.; Mojelsky, T. W.; Lown, E. M. *Fuel* **1992**, *71*, 1355.

10.1021/ef990225z CCC: $19.00
Published on Web 03/23/2000

4−10 fused rings. Scanning tunneling microscopy on asphaltenes[14] image the aromatic portion of the molecule and show the largest dimensions of the aromatic ring systems are ∼11 Å, which is comfortably in this range. The results are consistent with X-ray scattering measurements of the size of stacked rings.[15] The recent mass spectra studies yield maximum ring systems in this range.[11] NMR results also indicate the average number of rings in a single fused ring system is around 7.[16] Optical absorption[17,18] and fluorescence emission spectroscopy[17,19] support this range for ring systems. There is no measurement which concludes that there are very large numbers (∼20) of fused rings per aromatic ring system.

Thus, if the very large molecular weights for asphaltene molecules are correct, then each molecule must have many separate fused ring systems. A recently proposed structure for an asphaltene molecule has 18 separate ring systems.[13] If small molecular weights are correct, then each molecule has only 1 or perhaps 2 ring systems per molecule. If one can determine that there is only one ring system per asphaltene molecule, this would indicate small molecular weights are correct.

In a recent paper, we established that fluorescence depolarization can be used to determine the absolute size of asphaltene molecules.[20] The diameters of asphaltene molecules were found to be 10−20 Å. Model compound analysis shows that this size range corresponds to approximately 500−1000 amu, in agreement with the mass spectroscopy results. Fluorescence depolarization studies are performed on extremely dilute solutions, thus they do not suffer from aggregation. More importantly all of the asphaltene sample is analyzed, precluding possible exclusion of the high-mass fraction. In addition, these results show a strong correlation of the size of the fused ring system with the size of the entire molecule. This correlation can hold only if the molecule contains one or two fused ring systems per molecule. This measurement independently confirms that the molecular weights are relatively small.[20]

In this Paper, we extend the fluorescence depolarization technique to survey the molecular size of a broad range of asphaltenes and related compounds. The general nature of our findings is established over this broad range of samples. Specific subtle differences for these samples are examined and related to known chemical properties. A dramatic size difference between coal and petroleum asphaltenes is found and corroborates previous findings.

II. Experimental Section

Our samples included a coal asphaltene graciously supplied to us by Professor M. Iino of Tohoku University, Japan. The bituminous coal sample was Tanito Harum from Indonesia. The sample was prepared from the coal liquifaction residue. The pyridine-soluble fraction was isolated, and its toluene-soluble fraction was then isolated; the *n*-hexane asphaltenes of this fraction were then collected.[21] The Arabian Medium Heavy vacuum resid *n*-heptane asphaltene[22] was supplied to us from Texaco by Dr. Eric Y. Sheu.

Asphaltene samples, defined here as heptane-insoluble−toluene-soluble, were prepared from crude oils from Kuwait (UG8), Kuwait (BG5), California (Cal), France (ST1). There was no processing of the crude oils prior to the separation of asphaltenes; these are virgin crude oils. This definition of asphaltene corresponds to the heaviest end of these crude oils; there was no oil component insoluble in toluene. The sample of the crude oil was mixed with *n*-heptane (40 cm^3/g). The resulting solution was stirred in the dark for 24 h and then filtered using a 1.2 μm pore size nylon Schleicher and Schuell filter. The precipitate was washed with hot *n*-heptane until the solvent wash was colorless. The resulting powder was air-dried. For all our virgin crude oil asphaltenes, we checked for effects from trapped resin or other oil components. Some of the asphaltene was then dissolved in toluene and reprecipitated again using a 40:1 volumetric ratio of *n*-heptane. After 24 h of stirring, the resulting precipitate was filtered and washed with hot *n*-heptane until the heptane wash was colorless. Furthermore, we note that the large heptane volume in this reprecipitation procedure was very light in color in all cases indicating that our original asphaltene sample had little if any contamination of materials soluble in *n*-heptane. In all cases, the original and reprecipitated asphaltene exhibit exactly the same rotational correlation times and spectra. There is no effect in our data from trapped resins and the like. The UG8 resin was obtained by precipitating the resin and asphaltene from the crude oil together with 40 cm^3/g of pentane added to the crude oil. The resulting precipitate was filtered and resuspended in 40 cm^3/g of *n*-heptane. After 24 h the heptane was filtered and taken to dryness leaving the resin. (This precipitated asphaltene was not used as it may contain occluded resin.)

The absorbances (A) of our solutions were measured using a CARY 500 UV−visible−NIR spectrometer. The absorbance of all solutions was kept below 0.2 to avoid complications from self-absorption (although the natural fluorescence red shift coupled with the decreasing absorption at longer wavelength for all asphaltenes mitigate this effect). In addition, at concentrations in the range of 0.06 g/L and higher, the decay curves exhibited additional anisotropy decay components which may be associated with dimer formation. Consequently, we maintained asphaltene concentrations at or below 0.025 g/L for analysis; typically we used the concentrations of ∼0.006 g/L. At these concentrations, our measured rotational correlation coefficients and our fluorescence lifetimes were independent of concentration. All rotational correlation times were determined at room temperature 19 °C in toluene with a viscosity of 0.59 cP. Two dyes, obtained from Aldrich Chemicals, were also used in this study, octaethyl porphyin (OEP) and a solar dye, *N*,*N*′-ditridecyl-3,4,9,10-perylenetetracarboxylic diimide; their structures are shown in Figure 1.

For collection of steady-state fluorescence spectra, we employed the (Photon Technology International) PTI C-72 + A-720 fluorescence spectrometer using a 75 watt Xe compact arc lamp source. Time-dependent fluorescence depolarization data were collected with the PTI C-72 system which employs a PTI GL-3300 nitrogen laser source along with a PTI GL-302 high-resolution dye laser with a fiber optic coupling to the measurement cell to excite the fluorescence. Figure 2 shows a schematic of this system. The directions of the excitation and emission light from the cell are oriented 90° from each other

(14) Zajac, G. W.; Sethi, N. K.; Joseph, J. T. *Scan. Microsc.* **1994**, *8*, 463.
(15) Pollack, S. S.; Yen, T. F. *Anal. Chem.* **1970**, *42*, 623.
(16) Calemma, V.; Iwanski, P.; Nali, M.; Scotti, R.; Montanari, L. *Energy Fuels* **1995**, *9*, 225.
(17) Mullins, O. C. Chapter 2, ref 6.
(18) Mullins, O. C.; Mitra-Kirtley, S.; Zhu, Y. *Appl. Spectrosc.* **1992**, *46*, 1405.
(19) Ralston, C. Y.; Mitra-Kirtley, S.; Mullins, O. C. *Energy Fuels* **1996**, *10*, 623.
(20) Groenzin, H.; Mullins, O. C. *J. Phys. Chem. A* **1999**, *103*, 11237.
(21) Iino, M.; Takanohashi, T. Chapter 6, ref 6.
(22) Sheu, E. Y.; Storm, D. A. Chapter 1, ref 5.

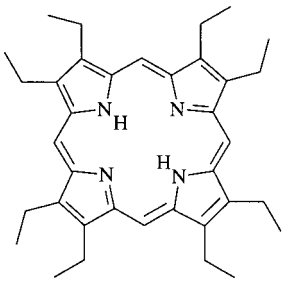

Octaethyl Porphine

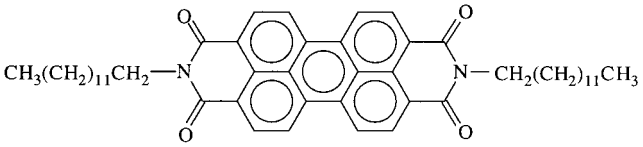

Solar Dye

Figure 1. Structures of dye compounds used for comparison with asphaltene molecules.

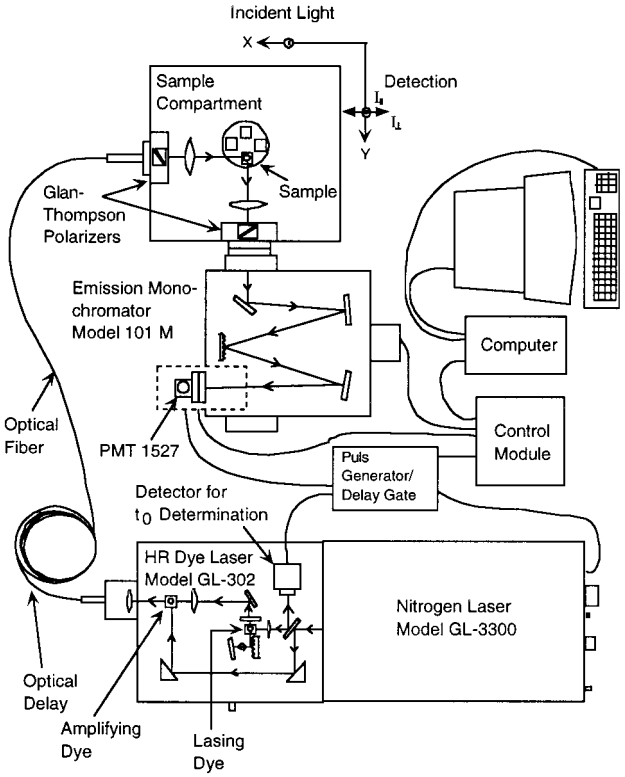

Figure 2. Schematic of experimental apparatus for collection of fluorescence depolarization decay curves.

with vertical polarization defined to be perpendicular to this plane.

For depolarization measurements, the wavelength of the PTI model 101M emission monochromator is fixed while two Glan-Thompson polarizers are used to select the polarizations. One polarizer is placed at the output of the fiber optic, immediately before the measurement cell, and the other polarizer is placed at the entrance to the emission monochromator. Fluorescence time decay curves are collected for four polarizations; vertical on the source side, vertical on the emission side (v−v), vertical−horizontal (v−h), horizontal−vertical (h−v), and horizontal−horizontal (h−h). The laser firing triggers a box car delay gate which then triggers a high voltage pulse at known delay to the PMT (photomultiplier). The short duration of the high voltage pulse "turns on" the PMT for a short time interval. The integrated current over this time interval from the PMT is detected. The delay time is sequentially scanned over the desired time range providing the fluorescence decay curve. The time resolution of the system is about 80 ps. A complete data set for one excitation and emission wavelength pair corresponds to acquisition of the four polarization combinations mentioned above. Typically, the total acquisition time for the four curves is 2 h. Reproducibility of signal levels was checked periodically during the acquisition time to validate the data. In addition, the v−h and h−h curves should overlay again allowing for excellent quality control. Duplicate (or more) runs were performed for all wavelength pairs to ensure precision. Typically, χ-square values of 1.2 or less were obtained for a good run.

III. Theory

In the following we will assume a spherical molecule rotating in a viscous medium subject to a sticking boundary condition. The following definitions are used:[23]

$$D(t) = I_{||}(t) - I_{\perp}(t) \tag{1}$$

$$S(t) = I_{||}(t) + 2I_{\perp}(t) \tag{2}$$

and

$$r(t) = \frac{D(t)}{S(t)} \tag{3}$$

where $I_{||}(t)$ and $I_{\perp}(t)$ denote a detection of light linearly polarized parallel and perpendicular to the linearly polarized excitation and $r(t)$ represents the anisotropy of the fluorescence emission.

We will assume an experimental setup as depicted in Figure 2. The exciting light is propagating in the negative x-direction and its polarization is directed along the z-coordinate of a laboratory-fixed system. The fluorescence will propagate along the positive y-axis and the polarization will be detected either in z- or in x-direction. The origin is placed conveniently at the position of the fluorophore. The transition dipole moment $\vec{\mu}$ shall have an arbitrary orientation with respect to the molecule axes. While the orientation of $\vec{\mu}$ stays constant in the molecular frame, it is time dependent in the laboratory frame. The angles θ,ϕ define the orientation of $\vec{\mu}$ with respect to the laboratory frame. $W(\theta,\phi,t)$ denotes the probability that the vector $\vec{\mu}$ is oriented (θ,ϕ) at time t. The diffusion equation of the problem is written as[24]

$$\frac{\partial W(\theta,\phi,t)}{\partial t} = D\nabla^2 W(\theta,\phi,t) \tag{4}$$

in which D is the rotational diffusion constant. The probability $W(\theta,\phi,t)$ is determined to be

$$W(\theta,\phi,t) = \frac{1}{4\pi}[1 + 2e^{-6Dt}P_2(\cos\theta)] \tag{5}$$

The anisotropy is obtained as

$$r(t) = \frac{2}{5}e^{-6Dt} \tag{6}$$

(23) Wahl, P. In *Biochemical Fluorescence: Concepts*, Vol 1, 2; Chen, R. F., Edelhoch, H., Eds.; Marcel Dekker: New York, 1975; Chapter 1.

(24) Tao, T. *Biopolymers* **1969**, *8*, 607.

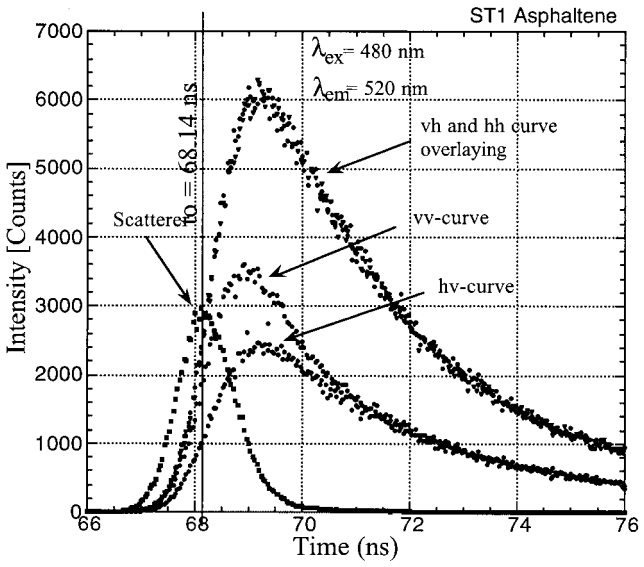

Figure 3. Unprocessed data for determination of fluorescence depolarization. The large separation of the vv and hv at early time, which then diminishes at later times, is due to rotational depolarization. The sample is ST1 asphaltene, $\lambda_{ex} = 480$ nm, $\lambda_{em} = 520$ nm.

Table 1. Aspect Ratio and Anisotropy Rotational Correlation Times for an Oblate Spheroid vs a Sphere with the Same Volume *V*[24]

$1/\rho$	$\tau_r/\tau_{r,sph}$
2	1.41
4	2.25

For a sphere, the diffusion tensor D reduces to a scalar D

$$6D = \frac{kT}{V\eta} \tag{7}$$

where η is the viscosity of the solvent. The decay time of the anisotropy $\tau_{r,sph}$, the parameter of our experiment, can now be written as[24]

$$\tau_{r,sph}^{-1} = \frac{kT}{V\eta} \tag{8}$$

Anisotropic Rotator. The more complex model of the anisotropic rotator can be treated completely in the operator formalism.[25] ρ is the ratio of the longitudinal semiaxis to the equatorial semiaxis of the ellipsoid. Table 1 lists the ratio of rotational correlation times for an ellipsoid versus a sphere, both having the same volume, for different aspect ratios $1/\rho$ of the oblate spheroid.

For a given rotational correlation time, the ratio of the calculated major axis of an oblate spheroid to the calculated diameter for a sphere goes as $(\tau_{r,sph}/\rho\tau_r)^{1/3}$.[26] The theory for the fluorescence depolarization decay of an anisotropic rotator has been presented and discussed in ref 26.

Data Fitting. Figure 3 shows typical data for a given wavelength pair, excitation at 480 nm and emission at 520 nm. The time zero for the dye laser pulse is at 68.14 ns. Typically, we used a wavelength shift of 40 nm between the excitation and emission to preclude any possibility of direct detection of scattered light, while still exciting and detecting emission from the lowest energy electronic state. The h−h and v−h curves overlay as expected. The large difference between the v−v and h−v curves at early times clearly shows a large anisotropy. This anisotropy decays at later times due to molecular rotation.

(25) Chuang, T. J.; Eisenthal, K. B. *J. Chem. Phys.* **1972**, *57*, 5094.
(26) Ref 20, and references therein.

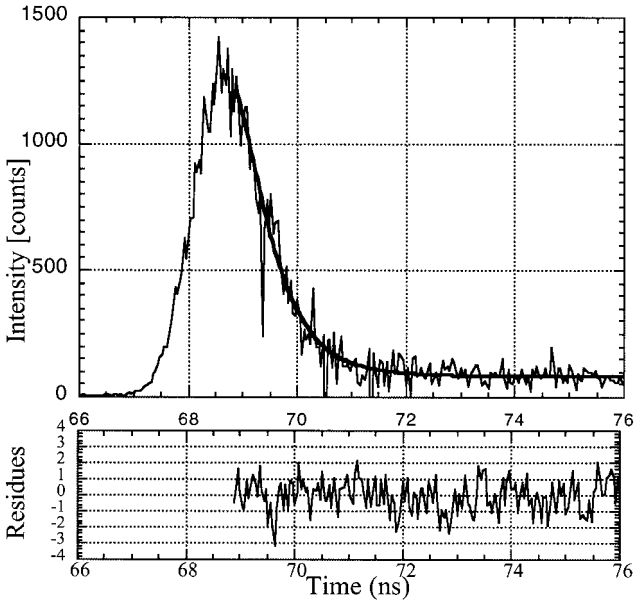

Figure 4. The difference curve $D(t)$ defined in eq 3. This curve dominates the time dependence of $r(t)$, the rotational anisotropy. The evident rapid rotational depolarization is due to the relatively small size of asphaltene molecules.

The v−h curve has a higher intensity than the v−v curve. This is due to the fact that horizontal and vertical polarized light have different transmission efficiencies through the emission channel of the instrument. This effect can be compensated by introducing a calibration factor, which is usually denoted with a capital G and is defined as $G = I_{hv}/I_{hh}$. Where I_{ij} refers to excitation with i polarization and emission with j polarization. All experimental data sets are corrected by multiplication of G with I_{vh}. I_{vv} then refers to $I_{\parallel}$, and $I_{vh}\cdot G$ to $I_{\perp}$.

Figure 4 shows the difference curve which was labeled $D(t)$ in eq 3 with its fitted value. For such short anisotropy decay times, the difference curve constitutes the main contribution to $r(t)$[20] and can be viewed to first approximation as the anisotropy curve. This fitting yields the rotational correlation time τ_r. Most of the decay curve is used for fitting, but not the earliest part because the early time behavior of the decay overlaps with the rising part of the laser excitation pulse producing a complex anisotropy curve which is not easily modeled.

IV. Results and Discussion

Figure 5a shows the rotational correlation times for a series of emission (and excitation) wavelengths for a series of asphaltenes obtained from virgin crude oils (ST1, UG8, BG5, Cal), vacuum resid (Resid), and coal (coal). The corresponding fluorescence emission spectra are plotted in Figure 5b to show the spectral range relevant to asphaltenes. The absolute correlation times are rather small, indicating the asphaltene molecules are not so large. As a reference we plot in this figure

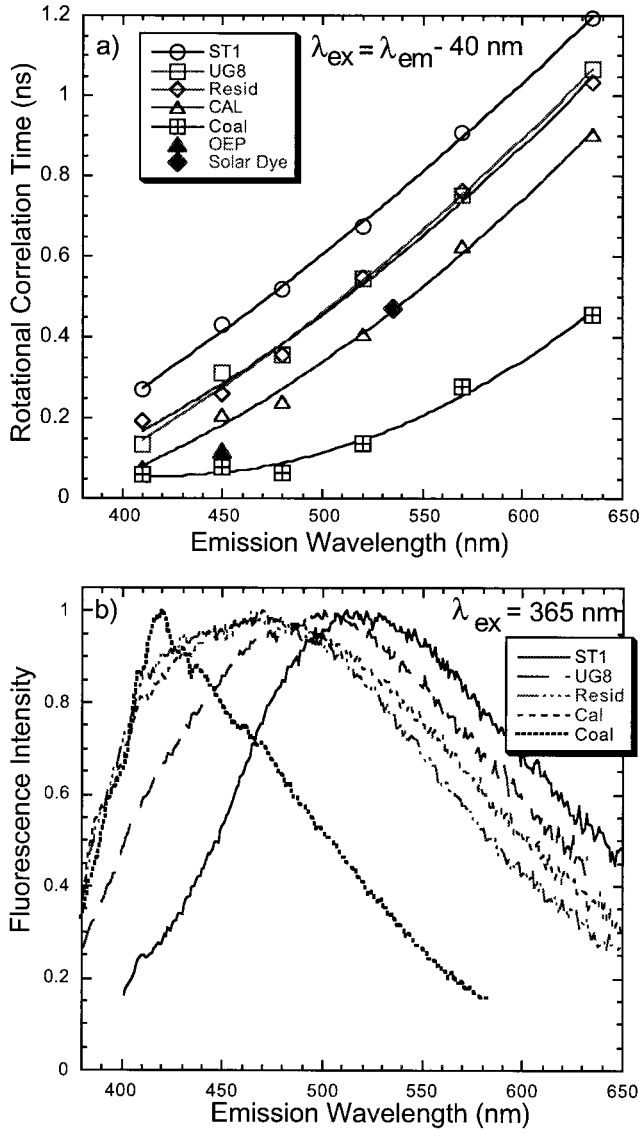

Figure 5. Rotational correlation times (top) and fluorescence spectra (bottom) for a series of asphaltenes and for two dyes. Rapid rotation is the norm and comparable to dyes shown in Figure 2. The strong correlation between chromophore size (spectral range) and molecular size shows that asphaltene molecules possess only one or two chromophores.

the rotational correlation times of two model compounds whose structures are shown in Figure 1. These model compounds provide a direct comparison as to the size of asphaltene molecules. With this comparison, the middle of the asphaltene distribution is seen to correspond to solar dye, a molecular weight of about 750 amu.[20]

In these experiments, we use excitation and emission wavelengths to select the size of the fused ring system to be examined. There is a well-known relation between the size of an aromatic ring system (number of fused rings) and the location of the lowest energy electronic transition.[17,27] In accordance with a quantum particle in a box, the larger the aromatic ring system, the lower energy the electronic transitions; this is particularly evident for the lowest energy electronic transition of the

(27) Turro, N. J. *Modern Molecular Photochemistry*; Benjamin/Cummings Pub. Co.: Menlo Park, CA, 1978.

Table 2. Ring Number and Fluorescence Emission Maxima for a Few Aromatic hydrocarbons in *n*-Heptane

aromatic hydrocarbon	number of rings	HO-LU excitation [nm]	emission maximum [nm]
benzene	1	265	280
naphthalene	2	300	320
anthracene	3	380	390
tetracene	4	475	485
pentacene	5	580	590

chromophores which corresponds to the HO-LU (highest occupied−lowest unoccupied) molecular orbital gap. Table 2 lists the HO-LU gap and fluorescence emission wavelength of a few aromatics.

The cyclic arrangement of rings as opposed to the linear arrangement of rings tends to shift the transitions to higher energy. Nevertheless, the correlation holds that more fused rings generally yield red-shifted transitions;[28] benzene and graphite are the two endpoints exhibiting extreme spectral differences. Thus, the excitation and emission wavelength can be used to select a relatively small range of ring systems to be interrogated; the range corresponds to overlapping HO-LU absorption and emission spectra of ring systems with different numbers of rings.

Figure 5a also shows that there is a monotonic, order-of-magnitude increase in the rotational correlation time across the asphaltene spectral range. That is, there is a strong correlation between the size of the asphaltene chromophore given by the emission wavelength and the size of the molecule, given by the rotational correlation time. This correlation requires that asphaltene molecules have only one or two chromophores per molecule. If an asphaltene molecule possessed say 10 chromophores per molecule, then there would be no correlation between chromophore size and molecular size. A small chromophore attached to a large molecule would exhibit the slow rotational correlation time of the entire, large molecule. The fact that we measure fast rotation for small chromophores and a factor of 10 slower rotation for large chromophores means that these individual chromophores are an appreciable fraction of the asphaltene molecule. Thus, asphaltene molecules possess one or two chromophores per molecule on average. Because asphaltene chromophores are known to possess on average about 7 fused rings, this result independently establishes that asphaltene molecular weights are small.

Figure 5a shows the plot of rotational correlation times for many asphaltenes. For all petroleum asphaltenes, the size ranges of the asphaltene molecules are comparable. Even the resid asphaltene exhibits sizes comparable to the virgin petroleum asphaltenes. Asphaltenes exhibit many relatively uniform properties such as carbon,[1−6] hydrogen,[1−6] and nitrogen[29] chemical speciation and, of course, solubility. It is not so surprising that the molecular sizes and weights for different asphaltenes also exhibit uniformity. The two petroleum asphaltenes exhibiting the greatest differences are Cal and ST1, while UG8 asphaltene is about average.

(28) Acree, W. E., Jr.; Tucker, S. A.; Fetzer, J. C. In *Polycyclic Aromatic Compounds*, Vol. 2; Gordon and Breach Scientific Publishers: U.K., 1991.

(29) Mitra-Kirtley, S.; Mullins, O. C.; Chen, J.; van Elp, J.; George, S. J.; Cramer, S. P. *J. Am. Chem. Soc.* **1993**, *115*, 252.

Table 3. Wavelengths, Anisotropies, and Derived Diameters Assuming a Sphere and an Oblate Spheroid of Aspect Ratio = 2

λ_{ex}	λ_{em}	τ_{ST1} [ns]	τ_{UG8} [ns]	Ani_{ST1}	Ani_{UG8}	$Diam_{ST1}$ [Å]	$Diam_{UG8}$ [Å]	major $axis_{ST1}$ [Å]	major $axis_{UG8}$ [Å]
365	410	0.270	0.134	0.62	0.51	15.2	12.1	17.1	13.6
406	450	0.430	0.311	0.43	0.34	17.8	16.0	20.0	18.0
440	480	0.518	0.356	0.79	0.34	18.9	16.7	21.3	18.8
480	520	0.674	0.546	0.28	0.26	20.7	19.3	23.2	21.6
530	570	0.909	0.751	0.35	0.27	22.8	21.4	25.7	24.1
595	635	1.19	1.06	0.37	0.30	25.0	24.1	28.1	27.1

Table 4. The Derived Molecular Major Axis Diameters Presuming an Oblate Spheroid with an Aspect Ratio of 2 for Asphaltenes ST1, UG8, Cal, Coal, and for UG8 Resin

		molecular major axis diameters [Å]						
λ_{ex}	λ_{em}	UG8	ST1	CAL	coal	resin	OEP	solar dye
365	410	13.6	17.1	11.3	10.3	12.8		
406	450	18.0	20.0	15.7	11.4	15.3	13.0	
440	480	18.8	21.3	16.5	10.5	16.8		
480	520	21.6	23.2	19.6	13.7	18.8		22.1
530	570	24.1	25.7	22.7	17.3	22.2		
595	635	27.1	28.1	25.6	20.4	25.5		

Table 3 lists for ST1 and UG8, the rotational correlation time, anisotropy and diameters (assuming the spherical model and an oblate spheroid with an aspect ratio of 1/2).

Table 4 lists the derived molecular major axis diameters presuming an oblate spheroid with an aspect ratio of 2 for asphaltenes ST1, UG8, Cal, Coal, and for UG8 resin. The two dyes are also listed for comparison. These sizes are rather small implying small asphaltene molecular weights. The large variation of molecular size with chromophore size shows that each molecule has only one or perhaps two chromophores.

The petroleum asphaltene with the smallest rotational correlation times is Cal. Thus for a given spectral range, Cal molecular sizes tend to be toward the smaller end of the (narrow) range of sizes probed by a given excitation and emission wavelength pair. In addition, Cal asphaltene also has the shortest wavelength fluorescence maximum, also indicating that the Cal ring systems are on average smaller than for the other asphaltenes. X-ray absorption near edge structure studies on asphaltenes show that Cal asphaltene is anomalously high in its sulfoxide content. 44% of the sulfur in Cal is in the sulfoxide group, while typically asphaltenes possess only a few percent sulfoxide.[30] (Cal asphaltene is 3.75% S by mass.) Sulfoxide is a very polar group and as such limits the solubility of sulfoxide-containing molecules. It is known from a variety of studies that it is sulfide sulfur, not thiophene sulfur which oxidizes to the sulfoxide group[30,31] (perhaps for Cal via biodegradation or contact with meteoric water). The implication is that Cal ring systems are smaller because molecules with large rings and sulfoxide groups would become insoluble in toluene and thus be removed from the asphaltene fraction. These Cal asphaltene molecules are bidentate, the aromatic ring system and the aliphatic sulfoxide group both produce strong intermolecular interaction.

The coal asphaltene exhibits some fundamental differences from the petroleum asphaltenes. The fluorescence spectrum of the coal asphaltene is sharply peaked toward short wavelength indicating that its aromatic ring systems are much smaller than for the petroleum asphaltenes. In addition, the rotational correlation times for the coal asphaltenes are quite short. For the bulk of the fluorescence emission curve for coal, the correlation times are shorter than for OEP implying a mass of about 500 amu for the coal asphaltenes. We are unable to measure much lower correlation times, so our results for coal might be biased toward higher molecular weights. It is well-known that coal asphaltenes are smaller than petroleum asphaltene;[21,32] our results are consistent with this expectation. Coal asphaltenes have shorter alkane chains than petroleum asphaltenes. Thus the ring system stacking is less disrupted. Consequently, to be soluble in toluene, the coal asphaltenes must have smaller ring systems.

Figure 6a shows the rotational correlation times for UG8 asphaltene and UG8 resin, and Figure 6b shows the corresponding fluorescence emission spectra. The fluorescence spectra show that the resin chromophores are most numerous in the shortest wavelength range investigated here. Nevertheless, the fluorescence spectrum of the resins shows a long wavelength tail extending in the spectral range where asphaltenes are most prominent. The rotational correlation times of the resin molecules show exactly the same trends as those of the asphaltenes. As the resin chromophore grows, the molecular size grows; thus, there is only a single chromophore per resin molecule. This result is expected for resins and corroborates our interpretation of the comparable data for asphaltenes. At any given spectral location, the resin molecules are a little smaller than those of the asphaltene molecules; this is also quite reasonable. Nevertheless, there are some resin molecules which possess large chromophores and are quite large. The properties of resin molecules are seen to form a continuous distribution with asphaltene molecules, which is not surprising considering their subtle solubility difference.

We have used a porphyrin as a model compound for asphaltenes, in part because the rotational correlation of the porphyrin is comparable to the lower end of the petroleum asphaltenes. In addition, spectral features found in asphaltene absorption spectra can be assigned to porphyrins. Figure 7 shows the absorption spectra of three asphaltenes as well as VO OEP, Ni OEP, VO tetraphenylporphyrin (TPP), and Ni TPP, the Soret bands are quite evident at ~400 nm. We also show derivative of the asphaltene absorption spectra. The derivative spectra show features clearly associated with VO OEP and Ni OEP and not with the TPP porphyrins, indicating the asphaltene porphyrins are the β-octa-

(30) Waldo, G. S.; Mullins, O. C.; Penner-Hahn, J. E.; Cramer, S. P. *Fuel* **1992**, *71*, 53.

(31) Kelemen, S. R.; George, G. N.; Gorbaty, M. L. *Fuel* **1990**, *69*, 939.

(32) Yen, T. F. Chapter 1, ref 6.

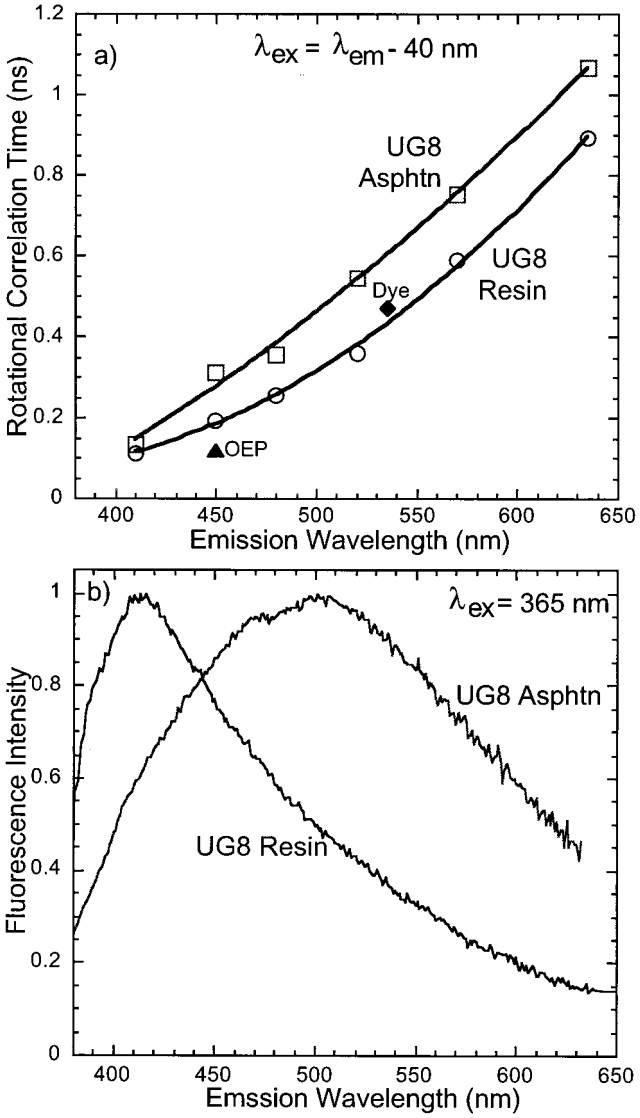

Figure 6. Rotational correlation times (top) and fluorescence spectra (bottom) for UG8 asphaltene and UG8 resin. The same absolute magnitudes and trends are evident for both samples, the resin molecular sizes grade continuously into the asphaltenes.

alkyl type. The heavy metal content of the three asphaltenes is listed in Table 5 and corresponds with the corresponding Soret band evident in the derivative spectra.

ST1 shows almost no Soret band and has a minimal content of V and Ni, BG5 has more V and shows the biggest feature corresponding to the VO OEP Soret band, while Cal has more Ni and has its biggest feature corresponding to the Ni OEP Soret band. It is known that asphaltene V and Ni are predominantly in porphyrin or porphyrin like compounds.[33] The use of a porphyrin model is certainly suitable for the lower end of the asphaltene molecular weight. A related, naturally occurring mineral is Abelsonite, a nickel(II) porphyrin (specifically deoxophylloerythroetioporphyrin, with all eight β-ring positions alkylated).[34] Furthermore, the rotational correlation time (thus derived size) we obtain

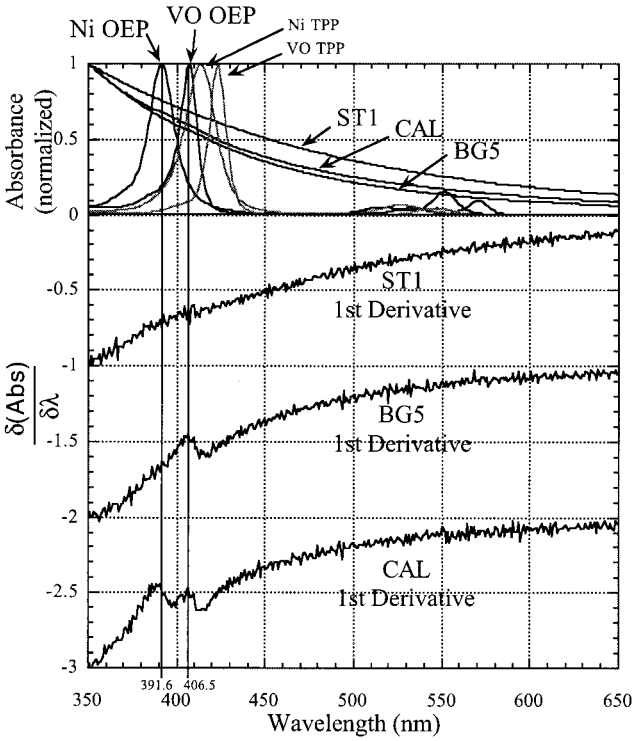

Figure 7. The absorption spectra and their first derivative for three asphaltenes. Ni OEP and VO OEP absorption spectra are also shown. The Soret bands of the porphyrins correspond to the peaks in the first derivative spectra of the asphaltenes in accordance with the metal content of the asphaltenes (Table 5). The asphaltene spectra coincide with OEP complexes, not the TPP complexes, supporting the β-octa-alkylated porphyrin assignment in the asphaltenes.

Table 5. V and Ni Content of Three Asphaltenes

asphaltene	V [ppm]	Ni [ppm]
ST1	2.6	8.5
BG5	438	141
Cal	141	632

here for OEP is 0.12 ns which is very close to the literature value for In OEP of 0.13 ns.[35] (The In central metal at the center of mass does not affect the correlation time.) We obtain the expected porphyrin size; our data indicate the presence of porphyrins in some of our asphaltenes,[33] and the asphaltene correlation times show that the size of the porphyrin is comparable to the smallest asphaltene molecules (present in quantity).

One important implication of the small molecular weights of asphaltenes (with the mean ~750 amu) is that there is very significant molecular heterogeneity in the asphaltene fraction. For idealized structures of much larger molecular weights, one can include many chemical functions in a single molecule such as metalloporphyrin, thiophene, sulfide, pyrrole, pyridine, various alkane chains, varied aromatics, etc. However, the small molecular weights of the asphaltenes preclude covalent linkages of such a large number of species. Thus, the variety of asphaltene molecules is huge, some with nitrogen, others with sulfur, some with a big ring system, others with a small ring system, an occasional molecule with a metal, a porphyrin, etc. At the risk of oversimplifying, we list in Figure 8 three idealized asphaltene structures which are consistent with a vari-

(33) Yen, T. F. *The Role of Trace Metals in Petroleum*; Ann Arbor Science Publishers: Ann Arbor, MI, 1975.
(34) Branthaver, J. F.; Storm, C. B.; Baker, E. W. *Org. Geochem.* **1983**, *4*, 121.
(35) Mullins, O. C.; Kaplan, M. *J. Chem. Phys.* **1983**, *79*, 4475.

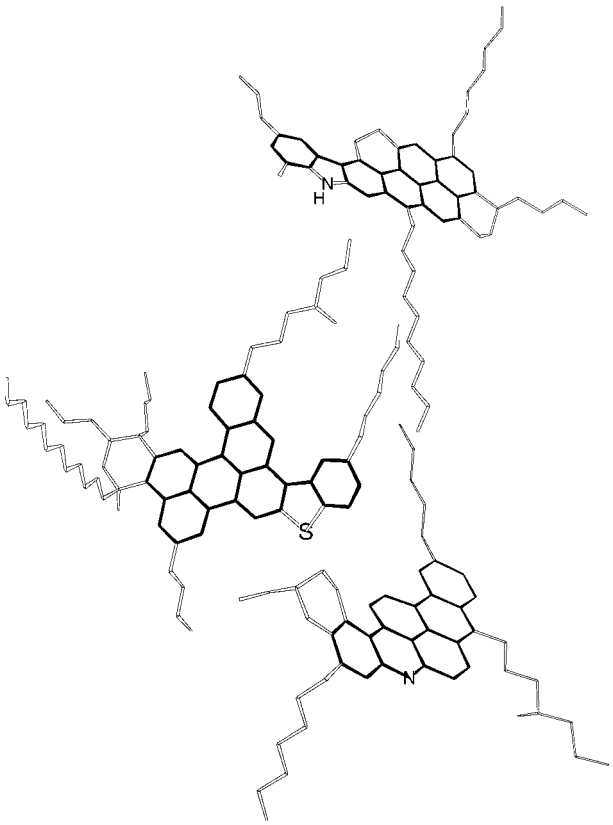

Figure 8. Idealized molecular structures for asphaltenes consistent with overall molecular size, aromatic ring systems, and chemical speciation. The aromatic rings are shown with darker lines.

ety of data including the aromatic fraction for carbon,[1−6] the $-CH_2-$ to $-CH_3$ ratio,[1−6] sulfur[30,31] and nitrogen speciation,[17,29] alkane structures,[13] and ring sizes and number of fused ring systems per molecule (determined herein).

One point of concern is the possible effect of energy transfer from one chromophore to another on our data. Intermolecular interaction is ruled out by the use of very low concentrations. For the concentration range used here, we found no change in either the rotational correlation constant or the fluorescence decay rate with changes in concentration. In addition, the fluorescence decay rates which are quite sensitive to intermolecular interaction, are found to be intrinsic; that is, they match dilute maltene decay rates.

Also of concern is intramolecular energy transfer from one chromophore to another within in a single molecule. Previously, various fluorescence studies have shown that strong intermolecular energy transfer occurs with crude oils and asphaltenes at sufficiently high concentrations.[17,36−38] This energy transfer results in a dramatic decrease in the lifetime of the initially excited chromophore and is quite evident for high concentrations.[38] A study designed to elucidate effects from intramolecular energy transfer or intramolecular quenching in asphaltenes reported that dilute solutions of asphaltenes and maltenes exhibit the same lifetimes across the UV and visible spectral range and concluded that no appreciable intramolecular energy transfer exists for asphaltenes.[39] Corroborative studies of alkyl dipyrenes show that dimer emission dominates for only a few chain lengths; generally, monomer emission dominates.[40] This result indicates that optimal chromophore configuration is required for strong intramolecular interaction. This flexibility would not be generally expected in an asphaltene molecule which possesses two chromophores; steric interactions are quite important in asphaltene ring stacking. Our large anisotropies seen in Table 3 also indicate that intramolecular energy transfer is not large because energy transfer with subsequent fluorescence greatly reduces anisotropy.

The issue of molecular aggregation or even of dimer formation plays an important role in the proper measurement of asphaltene molecular weight. We found that at concentrations >60 mg/L, the anisotropy curves begin to exhibit a second exponential decay;[20] this may be due to molecular complex formation. Recently, studies of thermal lensing in dilute asphaltenes in toluene found thermal diffusivity extrema at 50 mg/L; this was attributed to the onset of aggregation.[41] This result which is in concert with our results explains why such high molecular weights are found with concentrated asphaltene solutions. In these cases, aggregate weights are being measured.

V. Conclusions

We find small absolute sizes of asphaltene molecules. Further, we find that individual chromophores constitute an appreciable fraction of the asphaltene molecule; this indicates that there are only one or two chromophores per asphaltene molecule. This result has not been previously demonstrated and provides independent support for small molecular weights for petroleum asphaltene molecules (500−1000 amu). These important new results should help terminate the long-standing controversy about asphaltene molecular weights. As expected, we find coal asphaltenes are significantly smaller than petroleum asphaltenes. The smaller asphaltene molecular weights imply greater asphaltene molecular heterogeneity in that each molecule cannot possess many different functionalities; this may be operationally important as different asphaltene fractions can exhibit unique behavior. The smaller molecular weights also indicate lower energy barriers exist to break apart asphaltene micelles which may also have important operational implications.

Acknowledgment. We are greatly indebted to Professor Iino for supplying us with a sample of coal asphaltene. In addition, we are also greatly indebted to Dr. Eric Y. Sheu for supplying to us a sample of vacuum resid asphaltene.

EF990225Z

(36) Downare, T. D.; Mullins, O. C. *Appl. Spectrosc.* **1995**, *49*, 754; also published in SPIE Milestones Series Vol. MS 126, *Selected Papers on Laser Beam Diagnostics*; Hindy, R. N., Hunt, J. H., Eds.; SPIE Optical Engineering Press: Washington, D.C., 1996.

(37) Ralston, C. Y.; Wu, X.; Mullins, O. C. *Appl. Spectrosc.* **1996**, *50*, 1563.

(38) Wang, X.; Mullins, O. C. *Appl. Spectrosc.* **1994**, *48*, 977.

(39) Ralston, C. Y.; Mitra-Kirtley, S.; Mullins, O. C. *Energy Fuels* **1996**, *10*, 623.

(40) De Schryver, F. C.; Boens, N.; Put, J. *Adv. Photochem.* **1977**, *10*, 359.

(41) Acevedo, S.; Ranaudo, M. A.; Pereira, J. C.; Castillo, J.; Fernandez, A.; Perez, P.; Caetano, M. *Fuel* **1999**, *78*, 997.